IAC-17-C1.IP.11 x 41423

THE COMBINED LAMBERT-TISSERAND METHOD APPLIED TO THE SINGLE FLYBY PROBLEM

Davide Menzio[1], Camilla Colombo[1]

[1] Politecnico di Milano, Department of Aerospace Science and Technology, Milano, Italy
davide.menzio@polimi.it

Abstract. From the theorisation of the gravity assist, several methods have been used to design flyby trajectories. Depending on the gravitational model used, two categories of approaches can be identified. The multiple targeting method implements a -branch and bound architecture, which foresees: the subdivision of the overall trajectory in many legs connecting only one pair of planets at each time; the analysis of interplanetary trajectory in the two-body dynamics of the Sun; the modelling of the flyby and of the manoeuvre to switch from one leg to another from arrival and departure conditions at the planet of flyby obtained by two-body analysis of consecutive trajectories.

Energy method, instead, tackles such problem from a purely energetic point of view, considering the specific energy associated to the conic to identify reachable bodies and possible encounter conditions. The representative methods associated to this two approaches are the Lagrange solution for the Lambert problem in the two-body problem and the Tisserand Criterion in the Circular Restricted Three Body Problem (CR3BP).

Both approaches represent an essential tool for a complete preliminary design, although the refined trajectory must be determined through an iterative procedure in which the approximate solution of patched two-body problem is improved in a more complex dynamical model through optimisation algorithm that uses the dynamics as a black box.

This paper proposes an optimisation strategy which implements the targeting (phasing) resolution approach applied to a single fly-by design problem with a closer look to the energy. Preliminary solutions, found through the Lambert method, are refined in the CR3BP through an optimisation strategy based on an energetic approach which introduces an alternative formulation of the Tisserand parameter to describe constraint and cost functions.

Preliminary results show an improvement in term of performances with the respect of a classic optimisation scheme although more conservative constraints are included. This novel algorithm proves to be capable to solve the single flyby problem and to generate unique mostly continuous trajectories. Its verification was performed on a hypothetic future mission to Mars mission with a scheduled flyby at Venus.

I. INTRODUCTION

The golden age of space travel saw the birth of several successful interplanetary missions that pave the way to the exploration of the rocky planets, Jupiter and the Galilean moons, and Saturn. Since Mariner 10, all deep space missions were characterised by the implementation in the trajectory design of the flyby technique ascribed to Yuriy Kondratyuk. In his paper [1], he firstly described the influence of gravity of planets on the trajectory of a spacecraft and suggested the possibility of escape and capture by altering the probe velocity passing at considerably close distance from a massive body. In short,

the probe experiences a change of velocity both in terms of magnitude and direction as a result of the influence of the gravitational attraction of the flyby planet. Such effects can be modelled separately distinguishing the rotation of the relative velocity resulting between entry and exit conditions on the hyperbolic trajectory inside the sphere of influence and the vector sum of the relative velocity and the heliocentric one of the planet at the crossing of the sphere of influence.

Recent missions are characterized by a significant reduced budget which translated into an increase of the collaborations among the space agencies and into a critical cut of the number of deep space probes (i.e. Galileo, Ulysses, Cassini, New Horizon, Dawn and Juno) and, vice versa, an increased interest for rocky planets, Mercury and Mars, in particular, for asteroids (Hayabusa) and comets (Rosetta and Deep Impact) too.

In contrast, plans for future mission are foreseeing a return to deep space projects with the objective to discover past and possible current forms of life, to understand the formation and the aggregation of planets from the planetesimal disk and to investigate asteroid deflection and asteroid exploitation. Targets of interest, apart from Mars which is in the plan of colonisation, are Europa and its frozen ocean, Titan and its methane seas, Encedalus and Triton for the cryo-volcanism [2] but also asteroids from the main and the Kuiper belt. If these missions sound extremely ambitious, the available budget does not go hand to hand and could even decrease to a level that were never reached neither for missions to the rocky planets. Thus, it is clear how mission design places a dominant role in containing the mission cost.

This work, motivated by the renewed interest by the European Space Agency and the National Aeronautics and Space Administration for future missions to Mars, planetary moon system and asteroid, found inspiration in the project with a view of colonisation of the Red Planet and in the issues associated to undertake manned flight. Considering the vulnerability of the crew to radiation and to confinement in enclosed spaces, direct flight can be seen too risky and thus flyby at Venus must be considered to open additional launch windows.

In this work, the design of a hypothetic mission to Mars will be considered as a test case for the application of two different approaches:

- the classical two-body designed which implements an accelerated resolution of the Lambert problem achieved in the rotated frame which allows a closer view to phasing and a direct transformation of its results in the synodic reference of the flyby planet and patching of the two legs via infinite or peri-centre manoeuvres depending on the flyby models considered (zero-SOI or Patched Conic Approximation);
- a refinement of the two-body solutions in the Circular Restricted three(3)-Body Problem obtained by means of an alternative formulation of the Tisserand parameter.

The next section (II) presents the classical procedure to construct two-body trajectories connecting two points defined at given epochs and to stick them together designing manoeuvres at the flyby in the linked-conic approximation. The third sub-section (II.III) shows how the results of the Lambert method can be written in co-rotating quantities: fundamental for the design of peri-apsis manoeuvres (II.III) but necessary step for the optimisation (III.III), as well.

Section three (III) recalls the derivation of the Tisserand parameter and threats its extended formulation. Finally, a shooting method is used to optimise the results of Lambert problem and ensure patching in the CR3BP frame (III.IV). Preliminary results for a mission to Mars are presented in section four (IV).

The overall motivation of this work relies in the COMPASS project masterplan whose main objective consists in the understanding of the effect of orbit

perturbations in an interplanetary environment and their use for mission design.

II. TRAJECTORY DESIGN IN THE 2BP

II.I. Classical Lambert Problem

Dealing with flybys is a targeting problem in which the spacecraft trajectory is designed to intercept a moving object. From a design point of view, it is a tedious exercise as it requires to resolve several two-body boundary-value problems, one for each gravity assist that the mission is required to perform, plus one [3].

For each leg, a conic leg connecting initial and final points, P_1 and P_2, defined at a specific epoch, t_1 and t_2 respectively, must be determined. This is often referred as the Lambert problem. It was Lagrange who first derived an analytical result combining the time law with the Kepler equation:

$$\sqrt{\frac{\mu}{a^3}}\Delta t = E_2 - e\sin E_2 - \left(E_1 - e\sin E_1\right) \tag{1}$$

where μ is the standard gravitational parameter of the Sun, a and e are semi-major axis and eccentricity of the conic arc, E is the eccentric anomaly of P_1 and P_2 and Δt the total time of flight-

Eq. 1 can be rewritten into:

$$\sqrt{\frac{\mu}{a^3}}\Delta t = \alpha - \sin\alpha - \left(\beta - \sin\beta\right) \tag{2}$$

by adopting the following transformation scheme:

$$\left(E_1, E_2\right) \rightarrow \left(E_M = \frac{E_2 - E_1}{2}, E_P = \frac{E_2 + E_1}{2}\right) \tag{3}$$

$$\sin\varepsilon = e\sin E_P \tag{4}$$

$$\left(E_M, \varepsilon\right) \rightarrow \left(E_M = \frac{\alpha - \beta}{2}, E_P = \frac{\alpha + \beta}{2}\right) \tag{5}$$

Such allows to write:

$$\sin\frac{\alpha}{2} = \sqrt{\frac{s}{2a}} \quad \sin\frac{\beta}{2} = \sqrt{\frac{s-c}{2a}} \tag{6}$$

where c and s are the chord P_1P_2 and the semi-perimeter of the triangle $F^*P_1P_2$.

The semi-major axis, a, is determined resolving numerically the non-linear equation (Eq 2) and the terminal velocities can be computed as follow:

$$\begin{aligned} v_1 &= \left(A + B\right)u_c + \left(B - A\right)u_1 \\ v_2 &= \left(A + B\right)u_c + \left(A - B\right)u_2 \end{aligned} \tag{7}$$

where:

$$A = \sqrt{\frac{\mu}{4a}}\cot\frac{\alpha}{2} \quad B = \sqrt{\frac{\mu}{4a}}\cot\frac{\beta}{2} \tag{8}$$

and

$$u_1 = \frac{r_1}{r_1} \quad u_2 = \frac{r_2}{r_2} \quad u_c = \frac{r_2 - r_1}{c} \tag{9}$$

Over the years, several algorithms were made to improve generality, convergence, accuracy and efficiency, although the resolution procedure has similar approach in terms of invariants and iteration process.

In the single flyby mission considered, only two Lambert legs are required.

II.II. Flyby model

Such constructed flyby trajectories are defined in the so called zero-SOI-radius model in which the dynamics is governed uniquely by the primary attractor and the effect of the secondary ones appears at the interception with an instantaneous change of heliocentric velocity both in magnitude and direction.

These results must be reinterpreted in the Patched Conic Approximation which assumes a division of the problem in consecutive domains where the dynamics of the spacecraft is influenced by one single attractor at a time [4]. Considering the terminal velocities at the flyby planet defined with respect to the primary source of attraction, the Sun, the relative arrival and departure velocities at the target can be obtained from:

$$\begin{aligned} v_\infty^- &= v_2^{leg_1} - v_{body} \\ v_\infty^+ &= v_1^{leg_2} - v_{body} \end{aligned} \tag{10}$$

diminishing the heliocentric velocity resulting from the resolution of the Lambert problem (*leg*) of the heliocentric velocity of the flyby planet (*body*).
These describe two hyperbolic trajectories that in general do not match since they present different magnitude and direction [3]:

$$v_\infty^- \neq v_\infty^+ \tag{11}$$

A powered gravity assist is required to achieve the patching of legs. According to the theory [9], the minimum cost in term of delta-v is achieved by performing a manoeuvre at the common periapsis of the hyperbolae which can be determined by solving the nonlinear system:

$$\begin{cases} e_{1/2} = 1 + \dfrac{r_p v_\infty^{-/+2}}{\mu} \\ \sin\dfrac{\delta_{1/2}}{2} = \dfrac{1}{e_{1/2}} \\ \delta = \dfrac{\delta_1}{2} + \dfrac{\delta_2}{2} \end{cases} \tag{12}$$

where r_p is the periapsis and δ the turning angle:

$$\delta = v_\infty^- v_\infty^+ \tag{13}$$

Patching is ensured by selecting the asymptotic distance Δ such that:

$$\Delta_{1/2} = \frac{\mu}{v_\infty^{-/+2}} \cot\frac{\delta_{1/2}}{2} \tag{14}$$

Finally, the delta-v that must be applied at the periapsis equals the difference of the periapsis velocities:

$$\Delta v = \sqrt{v_\infty^{+2} + \frac{\mu}{r_p}} - \sqrt{v_\infty^{-2} + \frac{\mu}{r_p}} \tag{15}$$

Exploiting the properties of the hyperbola, Δ can be rewritten as:

$$\Delta^{-/+} = \frac{\mu}{v_\infty^{-/+2}} \sqrt{\left(1 + \frac{r_p v_\infty^{-/+2}}{\mu}\right)^2 - 1} \tag{16}$$

and it can be noticed that since Δ and δ depend uniquely on v_∞ and r_p, if the periapsis decreases below the pre-defined value identified by the mean atmosphere altitude:

$$R_{\min}^{flyby} = R_{body} + h_{atm} \tag{17}$$

an additional manoeuvre is required at ∞^- to rise the periapsis to the minimum allowed value.

If from a theoretical point of view, periapsis manoeuvre appears to be the most efficient, in term of feasibility, manoeuvre at infinite are preferred as they permit a "relaxed" execution.

Such resolution scheme is extremely useful in order to evaluate how the total delta-v is affected by the variation of the boundary conditions expressed in terms of epoch (T) of departure and arrival which define the time of flight. For a single flyby, determining the flight schedule that minimizes the total delta-v requires to solve as many Lambert problems as

$$\sum_{i=1}^{n_{body}+1} T_{dep}^{leg_i} T_{arr}^{leg_i} \tag{18}$$

while ensuring the match between arrival and departure condition between consecutive flybys. Even like that, the computational effort is huge and increases proportionally with the number of flybys.

II.III. Rotated and synodic frames

Depending only on geometric relations, the capability of the Lagrange algorithm, to find the correct results for the Lambert problems, is not affected if the initial conditions are computed in different reference frames, as long as they do not modify the geometry of the problem.

Considering a classical targeting configuration (with departure and arrival conditions assigned to the positions of a 1st, r_1 , and 2nd, r_2 , planet defined respectively at

time t_1 and t_2), the Lambert problem can be resolved in rotated frame (by performing a rotation of $r_1(t_1)$ and $r_2(t_2)$ about $r_1(t_2)$ or $r_2(t_1)$ without adulterating the geometry, see Figure 1).

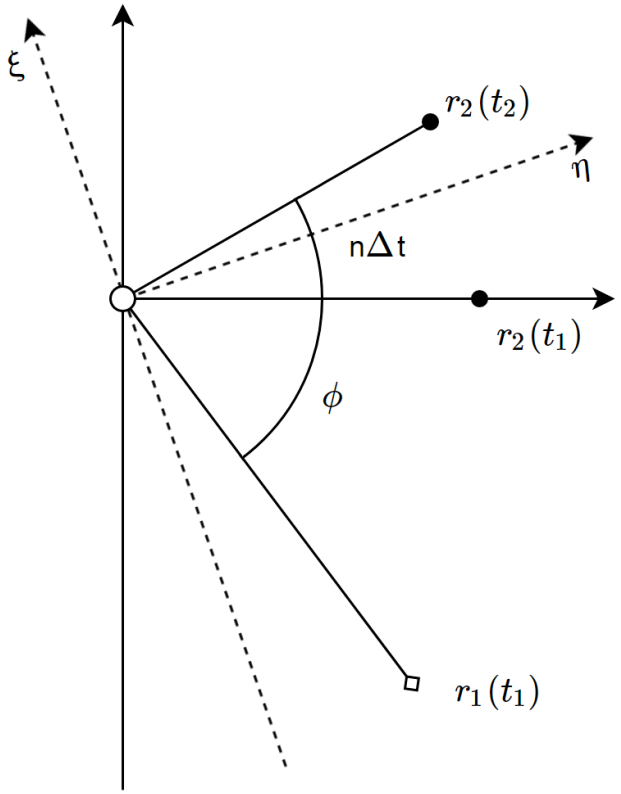

Figure 1: The rotated frame with the respect of $r_2(t_1)$

The use of the rotated frame presents some interesting properties since:

- it allows a closer look to the phasing as the angular distance between the terminal points and the x-axis depends only on the phase, ϕ, and the time of flight
- it is the halfway frame for the transformation of the sidereal reference in the synodic one, and thus permits a direct conversion in the co-rotating system.

Considering the shift of the origin from m_1 to the barycentre of m_1 and m_2, the rotation of $r_2(t_2)$ on $r_2(t_1)$ and the reduction of the velocities by the tangential contribute $\omega \times r$:

$$\begin{cases} r_1 = r_1(t_1) - \mu^* r_2(t_1) \\ r_2 = (1-\mu^*) r_2(t_1) \\ r_1 = v_1 - \omega \times r_1(t_1) \\ r_2 = R(-\mathrm{n}\,\Delta t) v_2 - \omega \times r_2(t_1) \end{cases} \tag{19}$$

results in the synodic frame, represented in Figure 2.

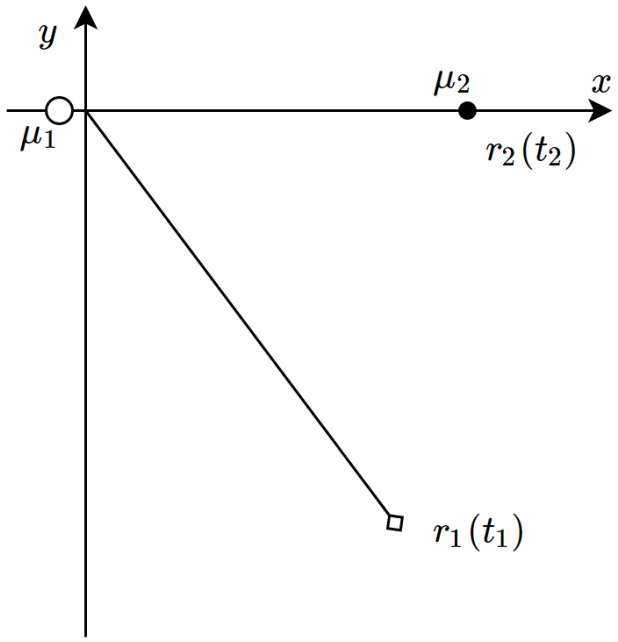

Figure 2: The synodic frame

The use of rotating quantities has several advantages in the context of:

- the design of two-body optimal manoeuvre which involves the patched conic approximation and the use of velocities relative to planet of flyby
- the optimisation of the two-body trajectories in the CR3BP that will be further discussed in the following paragraph.

In order to remain consistent with the synodic frame, the resolution of the Lambert with rotated terminal points must be initialised in such a way that the centre of rotation is preserved passing from a leg to another. In other words, the rotation must be performed about the

planet of the flyby, which for the first leg is associated to $r_2(t_1)$ but for the second to $r_1(t_2)$.

III. OPTIMISATION STRATEGY

The propagation of the Lambert two-body solution in the CR3BP does not result in a unique trajectory but shows gaps ranging from tens to hundreds of thousands of kms. Differently from the patched conic approach, the CR3BP presents continuous mixed dynamics which induce the two legs not to converge in a unique smooth orbit. A local optimiser implemented in MATLAB®, fmincon, has been selected to solve the problem of patching in the CR3BP.

Previous studies from Campagnola et al. [7] demonstrated that a reckless optimisation might converge to quasi-ballistic solutions which are not representable in the two-body design.

The definition of cost and constraint functions has a fundamental role in direct the convergence towards the desired result and thus must be wisely selected. The Tisserand parameter represents a suitable candidate to address the issues that previous studies identified.

III.I. The Planar CR3BP and the Jacobi Integral

The PCR3BP model, compared to the n-body problem, implements a simpler gravity field which, nevertheless, takes into account most of the perturbations experienced during a flyby trajectory.

The motion of a massless particle subjected to the gravitational attraction generated by two heavy masses rotating on coplanar circular orbits about their barycentre can be expressed in the co-rotating frame following [6]:

$$\begin{cases} \dfrac{d^2x}{dt^2} - 2\mathrm{n}\dfrac{dy}{dt} = \dfrac{\partial F}{\partial x} \\ \dfrac{d^2y}{dt^2} + 2\mathrm{n}\dfrac{dx}{dt} = \dfrac{\partial F}{\partial y} \end{cases} \qquad \begin{aligned} F &= \frac{\mathrm{n}^2}{2}\left(x^2+y^2\right) + \frac{\mu_1}{r_1} + \frac{\mu_2}{r_2} \\ r_1 &= \sqrt{(x+b)^2+y^2} \\ r_2 &= \sqrt{(x-a)^2+y^2} \end{aligned} \tag{20}$$

Where the mean motion, n, and the positions of the primary, a, and the secondary, b:

$$n = \sqrt{\frac{\mu_1+\mu_2}{l^3}} \qquad a = \frac{\mu_2}{\mu_1+\mu_2}l \qquad b = \frac{\mu_1}{\mu_1+\mu_2}l \tag{21}$$

are functions only of the fundamental distance between m_1 and m_2, l, and the mass parameter, μ^*:

$$\mu^* = \frac{\mu_2}{\mu_1+\mu_2} \tag{22}$$

III.II. The Tisserand Parameter

Considering the aforementioned dynamical system, the Jacobi's constant represents an integral form of the dynamics and constitutes the unique invariant of motion:

$$C = \mathrm{n}^2\left(x^2+y^2\right) + 2\left(\frac{\mu_1}{r_1}+\frac{\mu_2}{r_2}\right) - \left(\left(\frac{dx}{dt}\right)^2 + \left(\frac{dy}{dt}\right)^2\right) \tag{23}$$

The Tisserand parameter can be directly derived from the Jacobi's constant expressed in the sidereal quantities (ξ,η,ζ):

$$C = 2\mathrm{n}(\xi\eta - \xi\eta) + 2\left(\frac{\mu_1}{r_1}+\frac{\mu_2}{r_2}\right) - \left(\xi^2+\eta^2+\zeta^2\right) \tag{24}$$

under the assumptions of:

- small mass parameter: $\mu^* << 0$;
- large distance from the secondary: $r \approx r_1$;
- direction of the rotation of the primary and the secondary along z: $\mathrm{n}_{x,y} = 0$;

exploiting the definition of the angular momentum:

$$\xi\eta - \xi\eta = h\cos i \tag{25}$$

and the energy (vis-viva) equation:

$$\left(\xi^2+\eta^2+\zeta^2\right) = v^2 = 2\frac{\mu}{r} - \frac{\mu}{a} \tag{26}$$

which results in:

$$C = \mu_1\left(\frac{1}{a} + 2\sqrt{\frac{a\left(1-e^2\right)}{l^3}}\cos i\right) \tag{27}$$

that normalised by the heliocentric velocity of the secondary, gives:

$$\bar{T} = \frac{1}{\bar{a}_P} + 2\sqrt{\bar{a}_P\left(1-e_P^2\right)}\cos i_P \tag{28}$$

Such quantity is expressed in term of the normalized semi-major axis, *a*, eccentricity, *e*, and inclination, *i*, computed with the respect of the primary. The Tisserand parameter has a fundamental importance: whether flyby induces an overall change of the Keplerian elements, it remains constants and constitutes an invariant property of an object undergoing to a close encounter with a planet. Moreover, it gives a quick estimate of the relative velocity at the encounter [7][8]:

$$\begin{aligned} &@r_p: \quad r \quad l \quad v \quad v_{r_p} \\ &C_{r_p} = 3\frac{\mu_1}{l} - v_\infty^2 \quad \bar{T} = 3 - \bar{v}_\infty^2 \end{aligned} \tag{29}$$

III.III. The augmented Tisserand Parameter

Under the assumption of large distances from the secondary, the application of the Tisserand parameter is only possible by introducing the Poincaré section in the negative x-axis as proposed by Campagnola et al [9], see Figure 3:

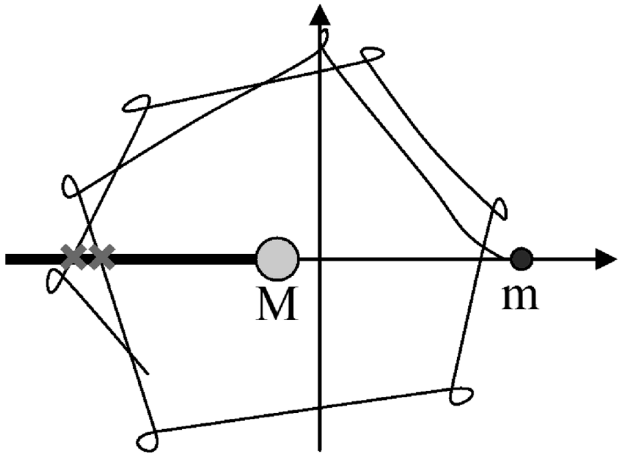

Figure 3: The identification of the positions where to estimate the Keplerian elements of the trajectory propagated in the CR3BP in order to compute the Tisserand parameter [9]

The use of the Poincaré section allows to identify a zone of confidence on the trajectory for the estimation of the Keplerian elements. Nevertheless, an unconstrained formulation could be more interesting from the point of view of the implantation and could have a larger field of application.

Now, Abandoning the assumption of large distance from the secondary, the Jacobi Integral transforms into:

$$C = M\left(\frac{1}{a} + 2\sqrt{\frac{a\left(1-e^2\right)}{l^3}}\cos i\right) - 2\frac{\mu_2}{r_1} + 2\frac{\mu_2}{r_2} \tag{30}$$

which normalized by the barycentric velocity of the secondary under the assumption of a small parameter gives:

$$\bar{T} = \frac{1}{\bar{a}_B} + 2\sqrt{\bar{a}_B\left(1-e_B^2\right)}\cos i_B - 2\frac{\mu^*}{r_1} + 2\frac{\mu^*}{r_2} \tag{31}$$

Comparing the new formulation of the modified Tisserand parameter (Eq.31) with the classical one (Eq.28). Two considerations can be made:

- Eq.5 introduces barycentric Keplerian elements instead of the classical heliocentric ones;
- it includes an additional numerical term expressed as function of the relative distances from the gravitational sources, primary and secondary, which allows the Tisserand to remain on average constant along the trajectory

III.IV. Local optimisation set up

The local solver, *fmincon*, belongs to the family of non-linear constraint optimisation technique. By varying terminal conditions via a shooting method, it minimises a given cost function in the domain where the constraints are satisfied. Intuitively, the algorithm converges to an optimal solution, if exists, moving towards the stationary in the admissible zone of the "cost-space" bounded by the constraints.

With the control variable assigned as the velocity at the terminal points, a classical optimisation propagates back and forward the refined terminal states in order to:

- patch the legs at the encounter with the flyby planet:

$$\left\| r_{enc}^{dep} - r_{enc}^{arr} \right\| < tol^* \tag{32}$$

- minimize the delta-v required by executing initial, mid-course and final manoeuvres:

$$\left\| v_1^{dep} - v_1 \right\|^2 + \left\| v_2^{dep} - v_2^{arr} \right\|^2 + \left\| v_3 - v_3^{arr} \right\|^2 \tag{33}$$

From the point of view of the algorithm, the dynamics remains "hidden" in the objective function, thus the selection of a cost and constraints functions which are directly connected to the system dynamics is extremely important.

The Tisserand parameter presents interesting properties which allows a wider use not only in the objective function but also in the constraints. Derived from the Jacobi constant, the Tisserand parameter describes the overall dynamic instead of the punctual representation given by the velocity. Introducing the Tisserand-Poincaré graph, which allows the representation of a heliocentric trajectory through its periapsis and apoapsis, it is possible to identify the quasi-ballistic (red) and pure ballistic (green) region of flyby see Figure.4. These zones are delimited by the level sets associated to the Tisserand parameter of $L_{4/5}$ and L_1 libration points, in particular:

- pure flyby occurs for:

$$T < T_{L_{4/5}} \tag{34}$$

- quasi-ballistic appears for

$$T_{L_{4/5}} < T < T_{L_1} \tag{35}$$

Thus, a new optimisation procedure can be designed in order to, not only, impose patching but also to force ballistic encounter. Moreover, the cost function can be rewritten in as:

$$K \left\| r_{enc}^{dep} - r_{enc}^{arr} \right\|^2 + \left\| v_1^{dep} - v_1 \right\|^2 + \left| T_{2-3} - T_{1-2} \right| \frac{M}{l} + \left\| v_3 - v_3^{arr} \right\|^2 \tag{36}$$

introducing the difference of velocity at the encounter through the dimensionalised Tisserand parameter and improving convergence by inserting in the objective function a scaled distance of the patching.

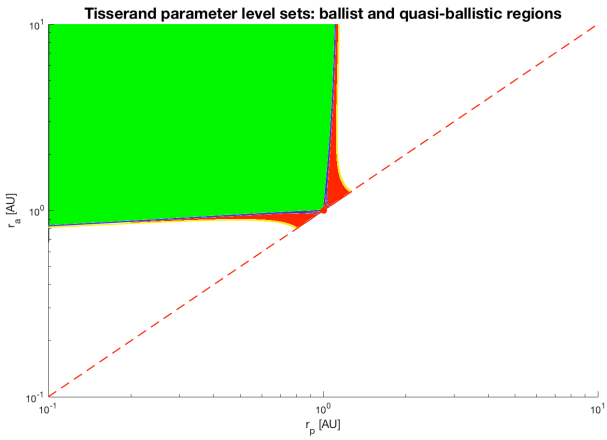

Figure 4: The ballistic (green) and quasi-ballistic (red) regions identified by the Tisserand level sets of $L_{4/5}$ and L_1 libration points

IV. PRELIMINARY RESULTS

Considering the mission to Mars with a scheduled flyby at Venus, the two-body design strategy consists in the identification of all the possible trajectories that connect Earth, Venus and Mars in a given time period, constrained to a maximum of one-year mission. An optimal solution can be found by varying departure and arrival dates for the Earth-to-Venus and Venus-to-Mars Lambert problems and studying its effect on the total delta-v.

As said, "pork-chop plot" is an extremely useful tool which allows to intuitively visualise the minimum delta-v solution and produces a repetitive pattern which depends only on the synodic period. This can be done comparing the "pork-chop" plots of the first and second leg.

The resolution of the Lambert problem from rotated initial conditions results in synodic solutions from

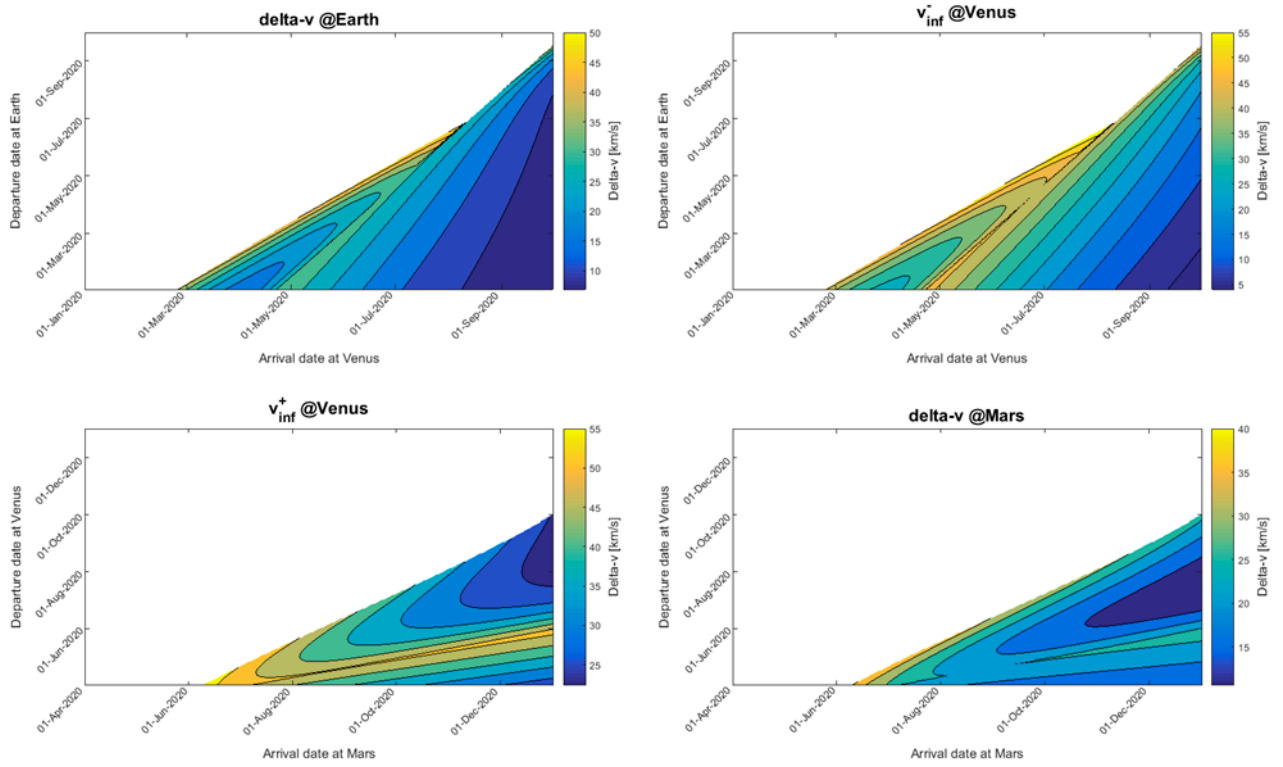

Figure 5: The results of Lambert problem in the synodic frame of Venus (the flyby planet): top-left and bottom-right graphs shows the delta-v for departure from Earth and arrival at Mars. Top-right and bottom-left plots are the equivalent ones for arrival and departure from Venus which can be directly related to the relative velocities at the planet and to flyby conditions

which the delta-v for the insertion onto the interplanetary trajectory at the Earth and for the capture at Mars, and the arrival/departure relative velocities at the encounter with Venus can be directly derived and represented in the "pork-chop" plots, see Figure 5.

Using the patched conic approximation and determining for each trajectory the optimal delta-v at the periapsis (Eq.15), over hundreds of thousands of flybys are obtained and results in the periapsis distribution, Fig.6.

Combining the delta-v at the periapsis with the one at the terminal points and re-arranging in term of the dates of departure from Earth and of arrival at Mars, the total delta-v can be represented in the combined "pork-chop" plot which groups all the minimum solutions and identifies the optimal delta-v, see Figure 7.

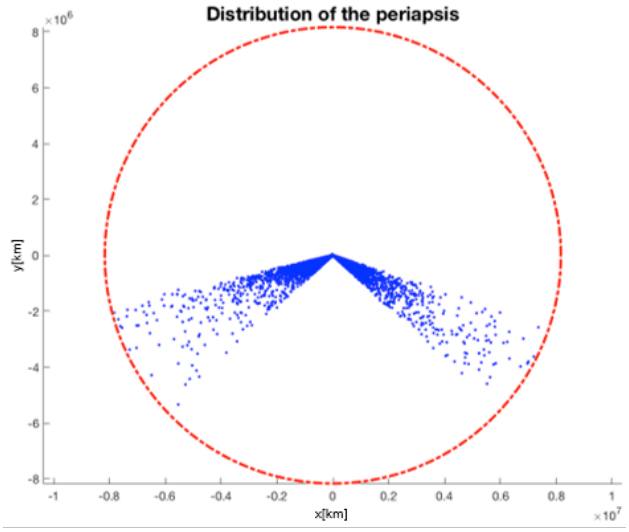

Figure 6: The periapsis position resulting from resolution of the system of (Eq. 12) with the relative velocities at Venus, see Figure 5

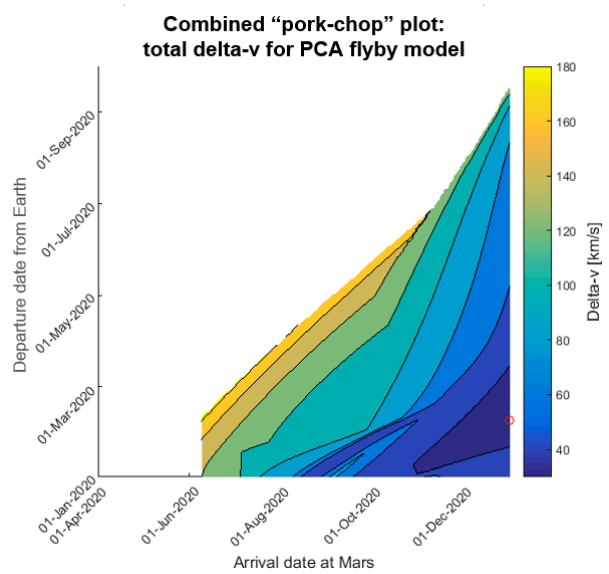

Figure 7: The total "pork-chop" plot combines the delta-v for departure from Earth and arrival at Mars (see Figure 6) with the delta-v at the peri-apsis obtained from (Eq.15)

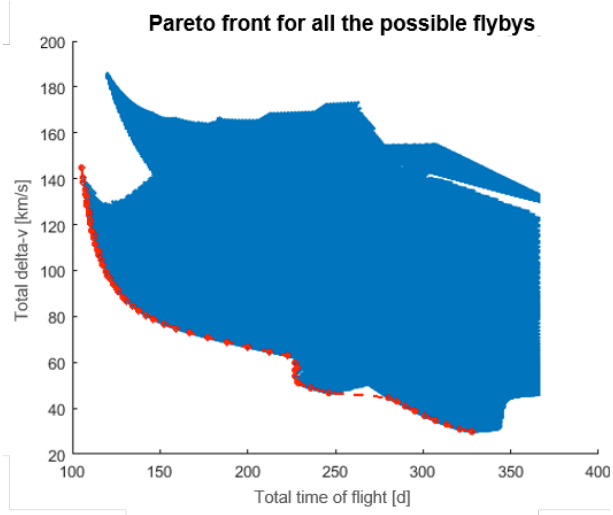

Figure 8: The pareto front resulting from the results of the combined "pork-chop" plot (see Figure 7) displayed in terms of minimum total delta-v and minimum total time of flight

Pareto front (see Figure 8) can be used to select optimal solutions not only in terms of minimum delta-v but also in term of minimum time of flight which are sampled in 51 points that ensures a good representation of the different minimization problems. Some of the most representatives cases, among the total 51 optimal points on the Pareto front, are reported in Table 1

Table 1: Seven equi-spaced points on the Pareto front

Dep@⊕	Flyby@♀	Arr@♂	Δv[km/s]	ΔT[d]
27-Jan-20	01-Jul-20	20-Dec-20	33.258	328
19-Jan-20	29-Jun-20	12-Nov-20	38.293	298
01-Jan-20	07-Mar-20	19-Jul-20	47.446	200
01-Jan-20	01-Mar-20	06-Jul-20	69.167	187
01-Jan-20	04-Mar-20	01-Jun-20	110.238	152
01-Jan-20	01-Mar-20	17-Apr-20	143.173	107
08-Jan-20	01-Mar-20	05-Apr-20	178.340	88

The efficiency of the optimisation algorithm is tested using the aforementioned results as initial guesses under the point of view of:

- convergence;
- number of iterations;
- number of function evaluations.

A minimum distance of patching is fixed at 50 km, small enough to be considered negligible given the involved distances. A scaling factor of $10^9 n^2$ (where n is the mean motion and it is used to scale distances on velocities) was selected as it ensures to initially magnify the distance at the encounter and to drive the search of the optimal solution towards the direction of patching but at the same time to nullify its effect once the constraints is satisfied, leaving the algorithm free to choose the minimum delta-v.

Preliminary results show that both optimisation strategies, at convergence, effectively generates an unique flyby trajectory, see Figure 9. Moreover, in most of the cases it can be shown that the energetic algorithm, which uses the modified Tisserand parameter, has better performances.

The repetition of classical and Tisserand optimisation for each initial condition, identified by 51 optimal points sampled uniformly on the Pareto front, leads to some conclusions

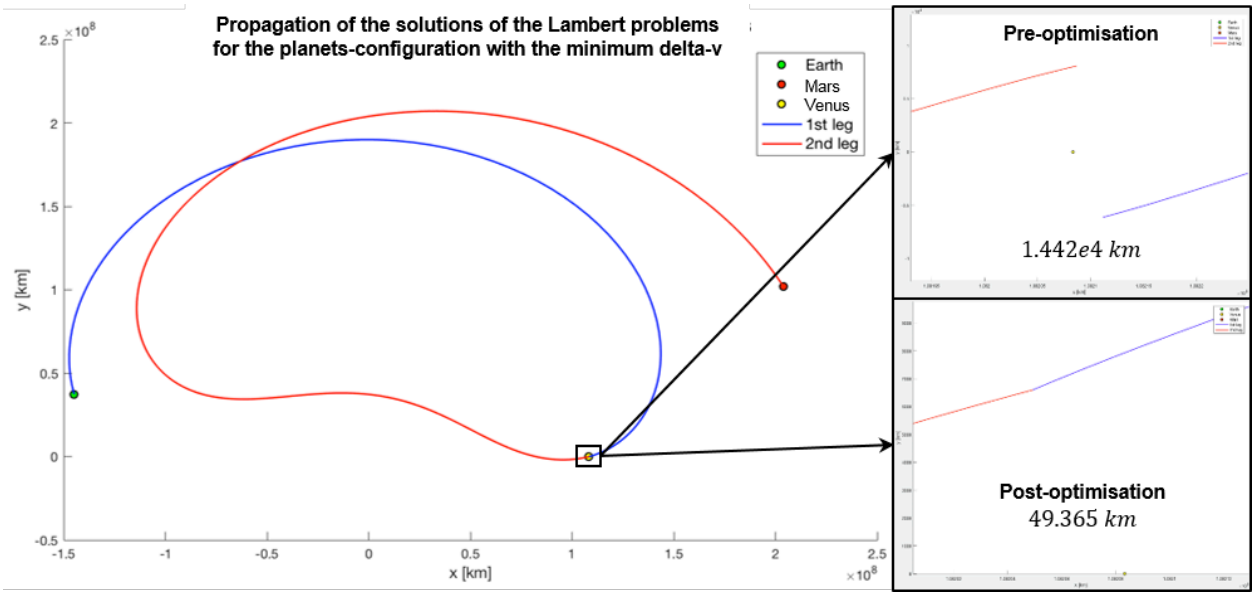

Figure 9: The difference between the overall trajectory propagated directly from the solution of Lambert problem (top-left) and from the optimised results (bottom-left)

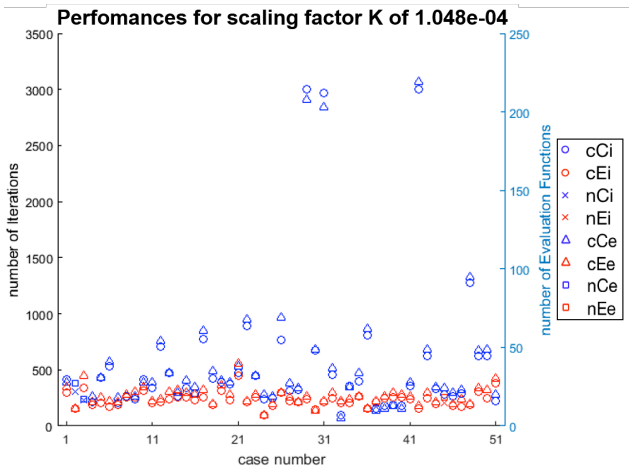

Figure 10: The performance of the classical (blue) and energetic (red) optimisation in terms of number of iterations and number of function evaluations, represented respectively with the circle, ◯, and with the triangle, Δ, markers in case of convergence and with the cross, X, and square, ☐, ones in the other

The number of iterations and the number of evaluation functions are represented for the two approaches using respectively the circle, ◯, and the cross, X, markers and the triangle, △, and the square, ☐, ones. Blue and red colours distinguish between classical and energetic methods, while ◯, Δ and X, ☐ inform whether the optimisation did or did not converge. As it can be seen, the energetic approach shows for most of the cases better performances in terms of both the number of iterations and the function evaluation, even though more conservative objective and constraints objective functions are implemented.

Through the T-P graph, it can be shown that a classical implementation of the optimisation might enter into quasi-ballistic region, while the energetic method cannot. At the same time, reversing the constraints, the algorithm might be forced to search for the optimal solution in the forbidden zone.

V. CONCLUSION

An analysis of the design for two-body flyby trajectories is presented and used to select optimal terminal conditions which are further optimised in the CR3BP. The classical Tisserand parameter is introduced and an unconstrained (in opposition to the standard whose application is constrained to negative x-axis, where the Poincaré section is fixed) equivalent

is presented. Two different approaches are considered in the definition of objective and constraints functions for the shooting method: the energetic strategy embeds the modified Tisserand parameter.

Preliminary results show that this strategy performs better in the majority of the cases despite more conservative constraints.

VI. FUTURE WORK

In future work, the calculus of variations will be exploited in the resolution of free time of flight/phasing problem and the preliminary design will be improved through the kick map model of the dynamics.

Advancement in the optimisation scheme will be made through the implementation of the Hamilton-Jacobi-Bellman equation for the design of optimal low-thrust trajectories in the CR3BP.

VII. ACKNOWLEGMENT

This project has received funding from the European Research Council (ERC) under the European Union's Horizon 2020 research and innovation programme (grant agreement No 679086 - COMPASS).

VIII. REFERENCES

[1] KONDRATYUK, Yuriy. V. To those who will read to build., 1938.

[2] TEAM and S. Roadmap., "Solar System Exploration– This is the Solar System Exploration Roadmap for NASA's Science Mission Directorate.," NASA Science Missions Directorate, Planetary Science Division, Washington, DC, 2006.

[3] PRUSSING, John E.; CONWAY, Bruce A. Orbital mechanics. Oxford University Press, USA, 1993.

[4] KOON, Wang Sang, et al. Dynamical systems, the three-body problem and space mission design. Free online Copy: Marsden Books, 2008.

[5] COLOMBO, Camilla; FERRARI, Fabio. Orbital Mechanics Notes. Politecnico di Milano, 2016

[6] SZEBEHELY, Victor; GREBENIKOV, E. Theory of Orbits-The Restricted Problem of Three Bodies. Soviet Astronomy, 1969, 13: 364.

[7] BATTIN, Richard H. An introduction to the mathematics and methods of astrodynamics., Aiaa, 1999.

[8] ROY, Archie E. Orbital motion. CRC Press, 2004.

[9] CAMPAGNOLA, Stefano; RUSSELL, Ryan P. Endgame Problem Part 2: Multibody Technique and the Tisserand—Poincaré Graph. Journal of Guidance, Control, and Dynamics, 2010, 33.2: 476.